Incomplete transfer of accessory loci influencing *SbMATE* expression underlies genetic background effects for aluminum tolerance in sorghum

Janaina O. Melo[1,2], Ubiraci G. P. Lana[1,2], Miguel A. Piñeros[3], Vera M. C. Alves[1], Claudia T. Guimarães[1], Jiping Liu[3], Yi Zheng[4], Silin Zhong[4], Zhangjun Fei[3,4], Lyza G. Maron[3], Robert E. Schaffert[1], Leon V. Kochian[3] and Jurandir V. Magalhaes[1,*]

[1]*Embrapa Maize and Sorghum, Road. MG 424, km 65, 35701–970, Sete Lagoas, Minas Gerais, Brazil,*
[2]*Departamento de Biologia Geral, Universidade Federal de Minas Gerais, Avenida Antônio Carlos 6627, 31270–901 Belo Horizonte, Minas Gerais, Brazil,*
[3]*US Department of Agriculture – Agricultural Research Service, Robert W. Holley Center for Agriculture and Health, Cornell University, Ithaca, NY 14853, USA, and*
[4]*Boyce Thompson Institute for Plant Research, Cornell University, Ithaca, NY 14853, USA*

SUMMARY

Impaired root development caused by aluminum (Al) toxicity is a major cause of grain yield reduction in crops cultivated on acid soils, which are widespread worldwide. In sorghum, the major Al-tolerance locus, Alt_{SB}, is due to the function of SbMATE, which is an Al-activated root citrate transporter. Here we performed a molecular and physiological characterization of various Alt_{SB} donors and near-isogenic lines harboring various Alt_{SB} alleles. We observed a partial transfer of Al tolerance from the parents to the near-isogenic lines that was consistent across donor alleles, emphasizing the occurrence of strong genetic back-ground effects related to Alt_{SB}. This reduction in tolerance was variable, with a 20% reduction being observed when highly Al-tolerant lines were the Alt_{SB} donors, and a reduction as great as 70% when other Alt_{SB} alleles were introgressed. This reduction in Al tolerance was closely correlated with a reduction in *SbMATE* expression in near-isogenic lines, suggesting incomplete transfer of loci acting *in trans* on *SbMATE*. Nevertheless, Alt_{SB} alleles from the highly Al-tolerant sources SC283 and SC566 were found to retain high *SbMATE* expression, presumably via elements present within or near the Alt_{SB} locus, resulting in significant transfer of the Al-tolerance phenotype to the derived near-isogenic lines. Allelic effects could not be explained by coding region polymorphisms, although occasional mutations may affect Al tolerance. Finally, we report on the extensive occurrence of alternative splicing for *SbMATE*, which may be an impor-tant component regulating *SbMATE* expression in sorghum by means of the nonsense-mediated RNA decay pathway.

Keywords: sorghum, aluminum tolerance, multi-drug and toxic compound extrusion family, transporter protein, alternative splicing, gene expression.

INTRODUCTION

Highly weathered soils such as those found in tropical and sub-tropical regions are frequently acidic, and, at pH values at or below 5.0, toxic forms of ionic aluminum (Al) are released into the soil solution, damaging root systems and inhibiting root growth, which in turn restricts water and nutrient uptake (Jones and Kochian, 1995; Horst *et al.*, 2010; Ryan *et al.*, 2010a). The resulting Al toxicity syndrome is one of the most important causes of yield reduction for crops cultivated on acid soils, which are widespread glob-ally (von Uexküll and Mutert, 1995; Kochian *et al.*, 2004). A widely investigated mechanism of Al tolerance involves the release of organic acids such as malate and citrate, medi-ated by transporters located in the plasma membrane of cells of the root apex (Kinraide *et al.*, 2005; Delhaize *et al.*, 2007). Once released into the rhizosphere, these organic compounds form stable, non-toxic complexes with Al, thereby providing a means for plants to withstand Al toxic-ity (Ma *et al.*, 2001; Kochian *et al.*, 2004, 2005).

The first Al-tolerance gene to be cloned in plants was *TaALMT1* (*Triticum aestivum* aluminum-activated malate

transporter), which encodes a transmembrane protein that mediates Al-activated malate efflux (Sasaki *et al.*, 2004). Additionally, transporter genes in the multi-drug and toxic compound extrusion (MATE) family confer Al tolerance via Al-activated root citrate release, as first shown in barley (*Hordeum vulgare* L.) (*HvAACT1*, Furukawa *et al.*, 2007) and sorghum (*Sorghum bicolor*) (*SbMATE*, Magalhaes *et al.*, 2007). Co-occurrence of both Al-activated malate and citrate release in *Arabidopsis thaliana* was shown to be due to members of the aluminum-activated malate transporter (ALMT) and MATE families (Liu *et al.*, 2009).

There is growing evidence indicating that additional loci modulate the expression of Al-tolerance genes, which may translate into epistatic interactions among Al-tolerance loci, converging to control a single, centralized physiological mechanism. For example, in Arabidopsis, both *AtALMT1* and *AtMATE* expression has been shown to be regulated by a C2H2-type zinc finger transcription factor, STOP1, which is also associated with tolerance to low pH (Iuchi *et al.*, 2007; Liu *et al.*, 2009). A homolog of STOP1, ART1, regulates the expression of a suite of genes related to Al tolerance in rice (*Oryza sativa*), including *STAR1* and *STAR2* (Yamaji *et al.*, 2009), *Nrat1* (Xia *et al.*, 2010), *OsALS1* (an ABC transporter involved in rice Al tolerance, Huang *et al.*, 2012) and the MATE family member *OsFRDL4* (Yokosho *et al.*, 2011).

In sorghum, Al tolerance and *SbMATE* expression were correlated in a set of lines previously known to possess various alleles at the Alt_{SB} locus on chromosome 3, which harbors *SbMATE* (Caniato *et al.*, 2007; Magalhaes *et al.*, 2007). Although a significant proportion of the Al tolerance variation has been shown to be controlled by factors present within the Alt_{SB} locus in certain segregating populations (Magalhaes *et al.*, 2004), the involvement of additional interacting loci acting across genetic backgrounds cannot be ruled out.

Here we show that near-isogenic lines (NILs) generated by marker-assisted introgression of various Alt_{SB} alleles retain varying degrees of Al tolerance in comparison to the original parents. The reduction in Al tolerance from parent to NILs may be very dramatic, reaching approximately 70%, depending on the Alt_{SB} donor line. This incomplete transfer of Al tolerance to NILs is associated with a reduction in *SbMATE* expression, emphasizing the importance of regulatory loci acting *in trans*. *Cis*-type regulation was found in two highly Al-tolerant sources, which are preferred donors of Al tolerance in sorghum. Allelic effects at Alt_{SB} resulting in variable Al tolerance were found to rely extensively on polymorphisms that are unrelated to protein structure, with regulatory polymorphisms greatly affecting Al tolerance. Finally, *SbMATE* alternative splicing is shown here to be a potentially important level of regulation, with a possible effect on sorghum Al tolerance conferred by *SbMATE*.

RESULTS

Physiological characterization of Al tolerance

Citrate release was assessed in eight sorghum lines (Figure 1) that were selected to represent a wide range of phenotypic responses to Al toxicity in sorghum (Caniato *et al.*, 2007). Based on previous data obtained at 27 μM Al^{3+}, these lines may be classified as Al-sensitive [BR007, BR012 and IS8577, with slightly higher relative net root growth (RNRG) in IS8577] or tolerant to Al toxicity (3DX, SC175, CMS225, SC283 and SC566) (Caniato *et al.*, 2007). Based on the RNRG at 39 μM Al^{3+}, SC283 and SC566 were highly tolerant to Al toxicity (Caniato *et al.*, 2007), and phenotyping at 60 μM Al^{3+} indicated that SC566 shows the highest level of Al tolerance (Caniato *et al.*, 2007, 2011). Citrate release in BR007 was extremely low at all Al^{3+} activities tested, consistent with its extreme degree of Al sensitivity. Citrate release in the remaining lines was activated by 11 μM Al^{3+} and inhibited at higher Al^{3+} activities, except in SC566. At 27 μM Al^{3+}, tolerant lines were able to maintain higher rates of citrate exudation compared to Al-sensitive lines. In the most Al-tolerant line, SC566 (Caniato *et al.*, 2007, 2011), its highest citrate release rate of approximately 600 pmol per plant per hour reached at 20 μM Al^{3+} was not inhibited even at the highest Al activity of 39 μM Al^{3+}. These results suggest that very high levels of Al tolerance in sorghum are related both to high rates of root citrate release and a lack of citrate release inhibition caused by high Al^{3+} activities.

Phenotypic characterization of Al tolerance in parents and derived NILs

The Alt_{SB} locus from the various donors was introgressed by marker-assisted selection, using BR012 (Al-sensitive) as the common recurrent parent, to generate NILs. Figure 2 shows that the NILs differed for Al tolerance based on RNRG, with the RNRG ranging from nearly 20–100%. Interestingly, a reduction in Al tolerance between tolerant parents and their respective NILs was observed in all cases, and the extent of this decrease was variable. The most pronounced reduction in RNRG was observed in NILs derived from 3DX (approximately 70%), SC175 (approximately 50%) and CMS225 (approximately 40%), whereas NILs derived from the most Al-tolerant lines, SC283 and SC566, were only 20% less tolerant than their respective parents, indicating extensive retention of Al tolerance by the parent alleles when introgressed into the BR012 genetic background.

Analysis of *SbMATE* expression

Figure 3(a) shows that Al exposure up-regulated *SbMATE* expression in the Al-tolerant lines CMS225, SC283 and SC566 by 1.5–3.2-fold, whereas *SbMATE* expression in other lines was repressed by Al. Interestingly, the lines
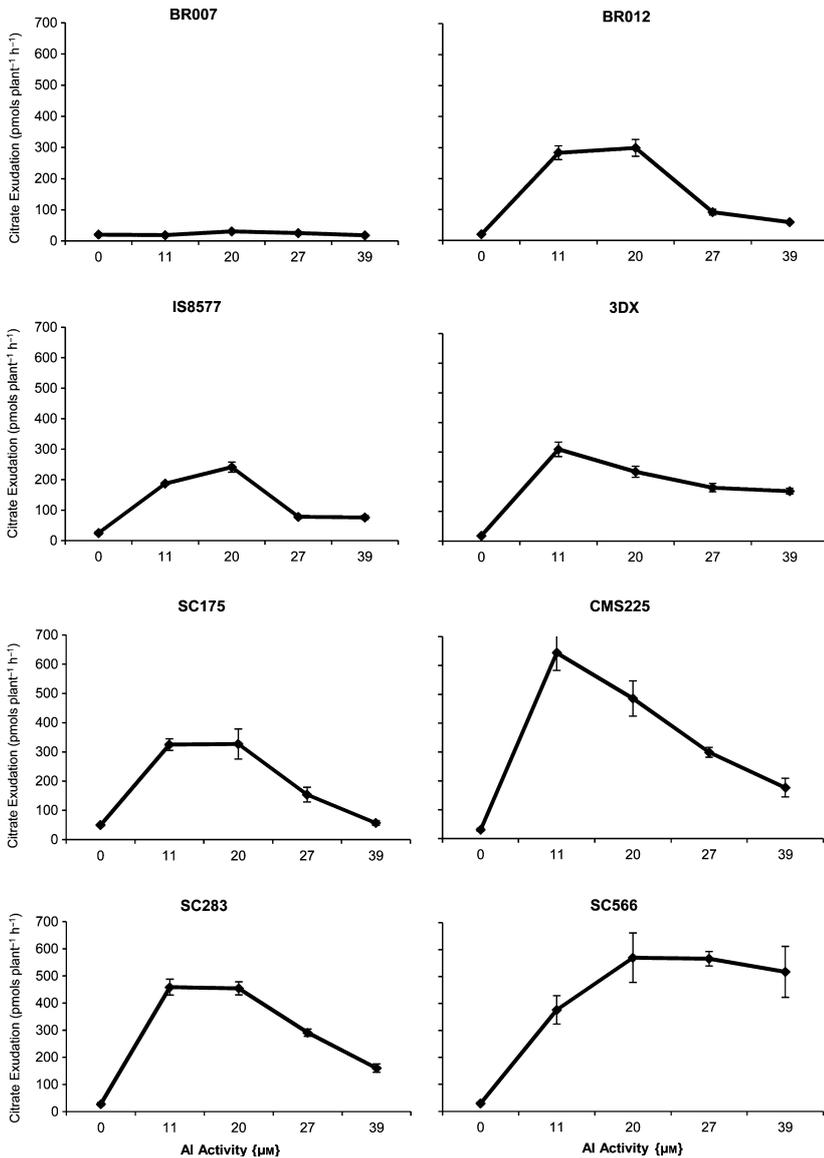
Figure 1. Root citrate exudation.
Sorghum lines (names shown at the top of each graph) were grown in nutrient solution pH 4.0 for 5 days under increasing Al^{3+} activities followed by exudate collection for 6 h. Values are means $\pm$ SEM of five replicates.

showing increased expression in response to Al are the most Al-tolerant lines (Caniato *et al.*, 2007), suggesting that Al up-regulation of *SbMATE* expression is related to specific changes in *cis* factors leading to high *SbMATE* expression and Al tolerance. In barley, at least in the basal root tip region, *HvAACT1* expression was apparently down-regulated by Al in the Al-sensitive cultivar Morex (Furukawa *et al.*, 2007), suggesting a degree of conserved functional evolution of *cis* factors controlling the expression of MATE genes. Interestingly, in all cases, *SbMATE* expression was lower in the NILs compared with their respective parents, consistent with the observed decrease in Al tolerance in the NILs. Comparing tolerant parents to derived NILs, the steepest decrease in *SbMATE* expression of approximately 80% was observed in 3DX, leading to very low expression levels comparable to those observed in the Al-sensitive lines. In

contrast, although reduced relative to the parents, *SbMATE* expression in the NILs derived from CMS225, SC283 and SC566 was still 25-, 60- and 70-fold higher, respectively, than the Al-sensitive line, BR012. This indicates that the significant retention of Al tolerance in these NILs was associated with high *SbMATE* expression in the donor alleles and a comparatively higher maintenance of *SbMATE* expression compared to other NILs such as that derived from 3DX. *SbMATE* expression and Al tolerance were moderately correlated in the parents (Figure 3b), but, within a common genetic background, this correlation increased to $r = 0.91$ in the NILs (Figure 3c).

Genomic structure and haplotype variation for *SbMATE*

Genomic sequences for *SbMATE* were obtained for 13 sorghum lines, including those used to generate NILs (Fig-

ure 4a,b). Eleven SNPs and one indel were found across the four *SbMATE* introns, with nine polymorphisms being found within the second intron of *SbMATE*.

In contrast, coding region polymorphisms were far more rare, being observed in only two lines, Tx642 and SC566, which were highly Al-sensitive (RNRG = 15%, Caniato *et al.*, 2011) and Al-tolerant, respectively. Exon 1 of Tx642
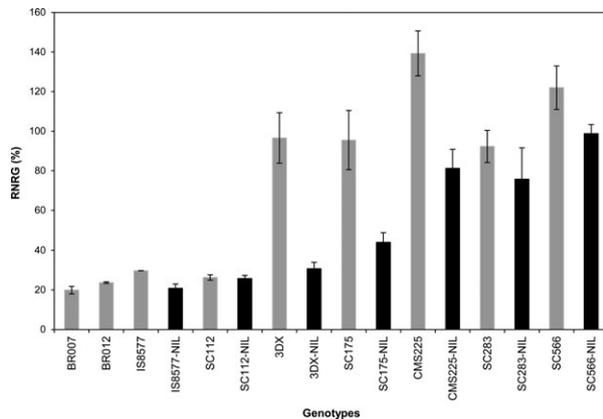
includes SNPs, insertions and deletions that create a premature stop codon, resulting in a truncated SbMATE protein with 241 amino acids. In SC566, a T→A change in the first exon of *SbMATE* resulted in a Leu→His substitution at amino acid position 261 of SbMATE. Protein domain analysis indicates that SbMATE is a member of the NorM-like subset of the MATE super-family. Structural predictions using the Phyre2 fold recognition server (Kelley and Sternberg, 2009) resulted in a 3D model structure (Figure 4c) with strong support for homology to the structure described for NorM from *Vibrio cholerae* (NorM–VC), the first and only MATE structure resolved to date (He *et al.*, 2010). The Leu→His substitution is predicted to occur at a helix (transmembrane domain 3, TM3) that does not line the internal cavity, but is peripheral towards the lipid bilayer. Within this helix, the His residue faces towards the outside surface of the molecule.

The potential effect of this substitution on functionality was assessed *in vitro* by heterologously expressing both the wild-type SbMATE (Leu at position 261) and the mutant SbMATE allele (SbMATE L261H, with His at position 261) in *Xenopus laevis* oocytes (Figure 5). Although cells expressing either SbMATE or SbMATE L261H showed significantly different electrical properties than non-expressing oocytes (i.e. control), the basic transport properties for the wild-type SbMATE did not differ from those of the mutant allele. Resting potential measurements in standard bath solution at pH 7.5 showed that cells expressing either variant were significantly more depolarized (approximately -20 ± 3 mV) than control cells (-59 ± 5 mV). Under voltage clamp conditions, oocytes expressing either SbMATE transporter showed significantly greater electrogenic

Figure 2. Aluminum tolerance in sorghum lines and respective near-isogenic lines (NILs) for *Alt_{SB}*.
The *Alt_{SB}* locus from the donor lines (gray bars) was introgressed by molecular-assisted backcrossing, using the Al-sensitive line, BR012, as the common recurrent parent, to generate NILs (black bars). The Al-sensitive and Al-tolerant standards BR007 and SC283, respectively, are included. Percentage relative net root growth (RNRG) is a standard measure of Al tolerance, and was determined after 5 days of treatment with 27 μM Al^{3+} in nutrient solution at pH 4.0. The RNRG (%) is calculated from root growth in Al divided by root growth without Al $\times$ 100. Values are means $\pm$ SEM of three replicates.
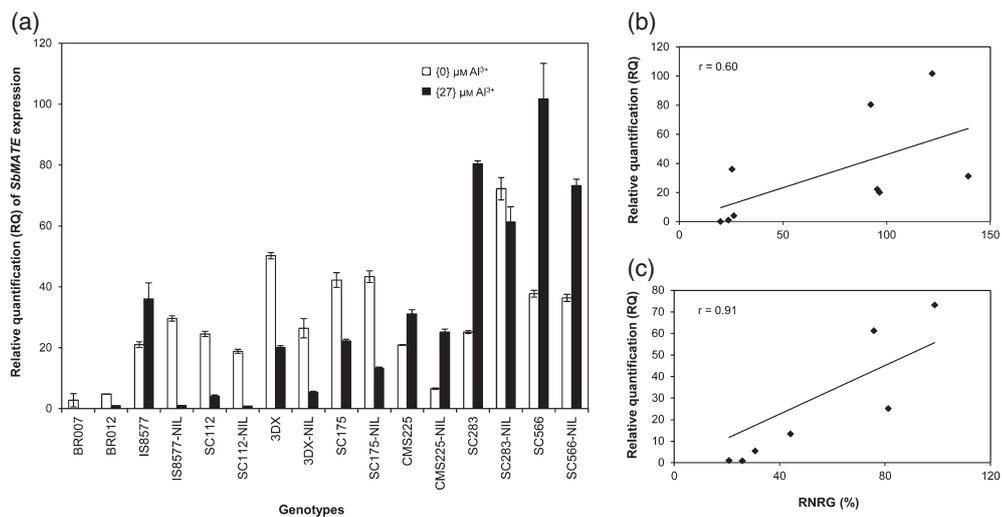

Figure 3. Expression analysis of *SbMATE*.
(a) Relative quantification of *SbMATE* expression was performed using seedlings grown in nutrient solution without (white bars) and with 27 μM Al^{3+} (black bars) at pH 4.0 for 5 days. The Al-sensitive and Al-tolerant standards BR007 and SC283, respectively, are included. Expression in the Al-sensitive line, BR012, treated with Al was used as the reference. Values are means $\pm$ SD of three replicates. (b, c) Correlation analysis between Al tolerance as determined by relative net root growth (RNRG) and *SbMATE* expression in (b) lines and (c) derived NILs.
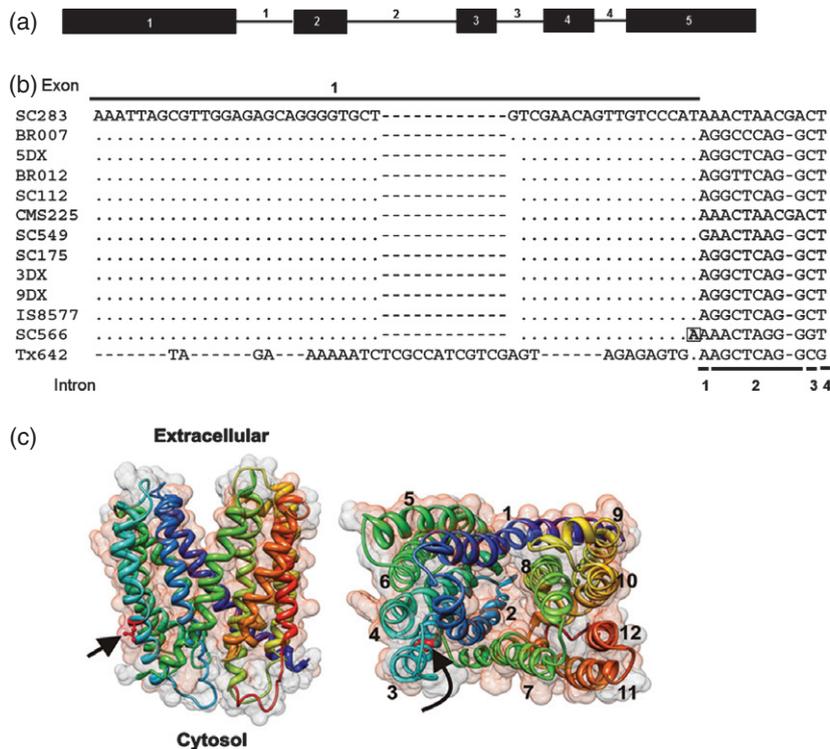
Figure 4. *SbMATE* haplotypes in 13 sorghum lines showing differential tolerance to Al.

(a) Genomic structure of *SbMATE*. The black boxes indicate five exons (numbered 1–5) interrupted by four introns (1–4).

(b) Partial alignment of *SbMATE* using CLUSTAL W, indicating polymorphisms. Thick lines above and below the alignments represent exons and introns, respectively, which are numbered sequentially as in (a). The A/T SNP in the first exon of SC566 is shown with the A allele present (box).

(c) 3D structural model (outward-facing configuration) of SbMATE based on structural homology. The model was generated by the Phyre2 fold recognition server (Kelley and Sternberg, 2009) using the NorM-VC MATE structure (He *et al.*, 2010) as a template. Left panel: Back view from the membrane side of SbMATE. with the extracellular and cytoplasmic sides indicated. Right panel: view from the outside of the cell. The internal cavity opens to the extracellular space and is occluded on the cytoplasmic side. Helices are colored using a rainbow gradient from N–terminus (blue) to C–terminus (red). The arrows indicate the location of the His residue 261 (colored in red with atoms represented as balls and sticks) in the third helix (TM3, shown in cyan). The molecule surface is shown as a transparency. The model does not take into account a longer loop region (approximately 70 amino acids) connecting the TM2 and TM3 helices, nor 95 residues constituting a cytoplasmic tail at the N–terminal end.

activity (i.e. negative currents) relative to the lack of activity elicited in control cells, with SbMATE-mediated currents reversing at holding potentials that were approximately 40 mV less negative than those observed in control cells (Figure 5a,b). Acidification of the bath media (from pH 7.5 to 4.5) resulted in a significant increase in the magnitude of SbMATE-mediated currents. In addition, increasing the cytosolic concentration of the organic anion substrate (i.e. citrate) resulted in a modest re-polarization of SbMATE-expressing cells, with resting potentials shifting from -20 ± 3 to -35 ± 5 mV. Under voltage clamp conditions, SbMATE-mediated currents remained pH-dependent. However, under these conditions, the SbMATE-mediated currents were apparently slightly greater than those recorded in the absence of cytosolic citrate. It is worth noting that, although smaller in magnitude, an endogenous conductance was observed in control cells micro-injected with citrate (Figure 5c, left panel). Overall, the electrophysiological analysis indicates that: (i) SbMATE mediates cation-coupled (i.e. proton-coupled) transport, typical of MATE transporters, and (ii) the Leu→His residue substitution at position 261 does not have a significant effect on the electrogenic characteristics of SbMATE transport, at least when expressed heterologously in *X. laevis* oocytes.

Alternative splicing of *SbMATE*

Because of the presence of intronic polymorphisms, primers were designed to amplify various regions of *SbMATE* in order to detect possible alternative transcripts. Amplification of cDNA samples using primers spanning intron 1 (Figure 6a,A) yielded a fragment of the same size as the 610 bp fragment amplified from genomic DNA (Figure 6a,B), in addition to the expected 494 bp fragment from cDNA with fully spliced intron 1 (Figure 6a,C). These results suggest the presence of alternative transcripts that possibly show complete retention of intron 1. In order to verify the presence of additional *SbMATE* isoforms, amplification was performed using primers that anneal to the first and
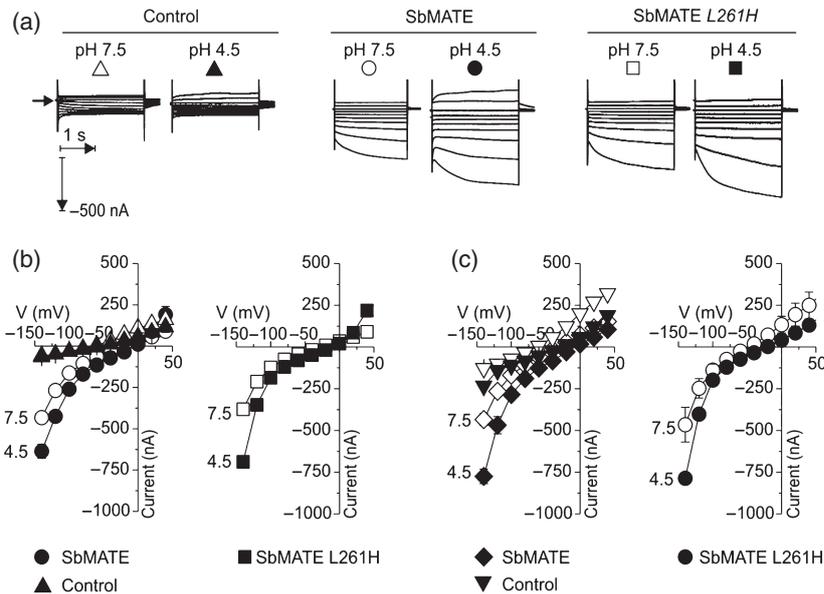
Figure 5. Electrophysiologically determined transport properties for wild-type SbMATE (with Leu at position 261) and SbMATE L261H (with His substitution at position 261) via expression in *X. laevis* oocytes using two-electrode voltage clamp.

(a) Examples of SbMATE- and SbMATE L261H-mediated currents elicited in response to holding potentials ranging from +40 to −140 mV (in 20 mV increments) in standard bath solution at pH 7.5 or pH 4.5, as indicated. Currents recorded in control cells (i.e. not injected with cRNA) are shown for reference. The horizontal arrow on the left margin of the traces indicates the zero current level. Time and current scales are given on the left.

(b) Mean current/voltage (*I/V*) curves constructed from steady-state currents recordings such as those shown in (a), for SbMATE (left panel) and SbMATE L261H (right panel) in standard bath solutions at pH 7.5 (open symbols) and pH 4.5 (filled symbols). For reference, values for non-expressing cells are shown in the left panel. The symbols correspond to those shown above the example traces in part (a). Values are means ± SD (*n* = 10 cells for each cRNA tested). The SEM is shown only when larger than the symbol.

(c) Mean current/voltage (*I/V*) curves for cells expressing SbMATE (left panel) and SbMATE L261H (right panel) in the presence of increased intracellular citrate. The intracellular citrate activities were increased by pre-loading the cells via micro-injection with 50 nl of 100 mM sodium citrate 2 h prior to electrophysiological recordings. Recordings were performed as described in (a) in standard bath solutions at pH 7.5 (open symbols) and pH 4.5 (filled symbols), and *I/V* curves were constructed as described in (b) (*n* = 6 cells for each cRNA tested).

last exons (Figure 6b). A 1638 bp fragment was observed in genomic DNA samples (Figure 6b,D), as expected based on the *SbMATE* sequence. Two bands were observed in cDNA templates. A weaker band, which was slightly larger than 1018 bp, was more visible in cDNA templates from the Al-tolerant lines SC566, SC283, SC175 and CMS225 (Figure 6b,E,F), although it was also faintly detected in Al-sensitive lines upon gel inspection. A stronger band with molecular size of 1033 bp, corresponding to the expected size of the fully spliced cDNA fragment, was also detected (Figure 6b,G). The cDNA bands were subsequently cloned and sequenced, confirming the presence of transcripts generated by alternative splicing. The molecular sizes for alternative transcripts retaining intron 1 were 610 (amplified using primers EXON–1R/EXON–2F, Figure 6a,B) and 1149 bp (amplified using primers EXON–1R/EXON–5F, Figure 6b,E), and that for those retaining intron 3 was 1126 bp (Figure 6b,F). These sizes exactly match the known genomic DNA sequence, confirming complete retention of introns 1 or 3. Sequencing of all genomic DNA bands in addition to the fully spliced *SbMATE* transcript (Figure 6b,G) also matched the expected sizes based on the *SbMATE* sequence.

RNA-seq (Figure S1) validated the isoforms retaining introns 1 or 3 described above. Strikingly, a previously unknown intron in the 5′ untranslated region (5′ UTR), and additional transcripts retaining each of the four *SbMATE* introns were also detected. The data also suggested the presence of partially retained introns, as seen for intron 2.

The predicted SbMATE proteins encoded by isoforms completely retaining each of the four introns were found to be truncated as a result of premature termination codons (Figure 6c). Thus, retention of introns 1–4 generates truncated SbMATE proteins ranging from 299 to 398 amino acids.

Expression analysis of *SbMATE* splice variants

We studied expression of the various splice variants of *SbMATE* using quantitative real-time PCR (Figure 7–a–d). Al-tolerant lines showed higher expression for all isoforms compared to the sensitive lines. For all isoforms, Al exposure either led to reduction or no dramatic change in the comparatively low *SbMATE* expression in Al-sensitive lines. Al up-regulation of *SbMATE* expression in Al-tolerant lines was clearly observed in CMS225 and SC283 for the
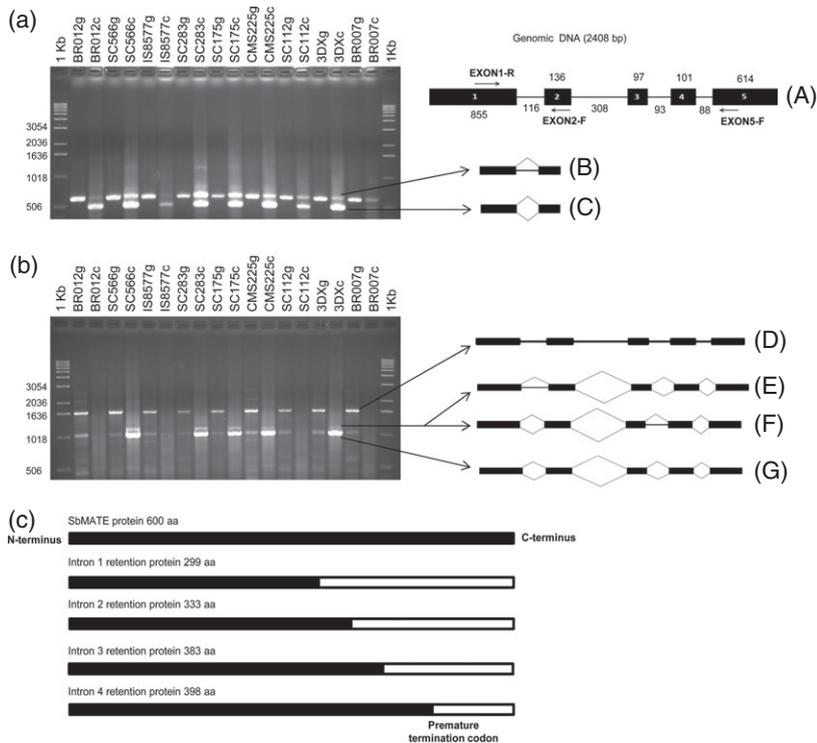
Figure 6. Alternative splicing of *SbMATE*.

(a) Amplification profiles of *SbMATE* genomic DNA (indicated as 'g' in genotype designations at the top of the gel image) and cDNA (indicated as 'c'), using primers EXON–1R and EXON–2F spanning intron 1. (A) Intron (thin lines) and exon (black boxes) structure of *SbMATE*, with numbers indicating sizes in bp and arrows representing primer binding sites; (B) 610 bp fragment containing unspliced intron 1 in cDNA samples; (C) 494 bp fragment corresponding to the fully spliced cDNA.

(b) Amplification profiles of *SbMATE* genomic DNA and cDNA using primers EXON–1R and EXON–5F. (D) 1638 bp fragment corresponding to genomic *SbMATE*; (E, F) 1149 and 1126 bp cDNA fragments with unspliced introns 1 and 3, respectively; (G) 1033 bp fragment of the completely spliced cDNA. Retained introns are depicted by single diagonal lines connecting exons, whereas normal splicing events are depicted by double diagonal lines connecting exons.

(c) Schematic depicting predicted proteins resulting from normal transcription and translation of the alternative splicing forms. The number of amino acids (aa) for each predicted protein is shown, in addition to the position of premature stop codons. Predicted molecular sizes are based on DNA sequencing.

isoform retaining intron 2 (i.e. the intron 2 isoform), whereas strong down-regulation of expression was observed in SC566 for the intron 2 isoform (Figure 7b). In fact, in the most Al-tolerant line, SC566, which also showed the highest level of *SbMATE* expression (Figure 3a), Al up-regulated *SbMATE* expression only for the intron 1 isoform, and expression in this line was strongly down-regulated for all other isoforms, particularly the intron 4 isoform (Figure 7d). A temporal analysis of expression under Al treatment focusing on the intron 1 isoform revealed a general time-dependent increase in expression, with much steeper increments in Al-tolerant lines, consistent with their higher levels of *SbMATE* expression compared to Al-sensitive lines (Figure S2). Finally, expression of the intron 1 isoform was assessed in both the parents and NILs to clarify a possible effect of the genetic background on alternative splicing (Figure S3). In general, both under Al treatment and control conditions, expression was higher in parents compared to the respective NILs. Expression of the intron 1 isoform in SC566 in the presence of Al was significantly higher than in the derived NIL. However,

this may reflect the reduction in *SbMATE* expression observed in the NIL in comparison with the high expression observed in SC566, rather than a genetic background effect on alternative splicing.

DISCUSSION

The genetic complexity underlying a target trait is essential information when predicting the effectiveness by which plant breeding strategies can lead to crop improvement. Accordingly, single major genes may be transferred to breeding lines by marker-assisted backcrossing to improve cultivars that were originally deficient in a given phenotype, with reasonable population sizes and in a timely manner. However, genetic background effects may represent a possible block in the path to improved crop performance on acidic, Al-toxic soils.

Here we report on extensive functional allelic variation present at the *Alt_SB* locus, which results in highly variable Al-tolerance phenotypes. We have shown that, in addition to the respective parents, derived NILs also exhibited different levels of *SbMATE* expression and Al tolerance. As
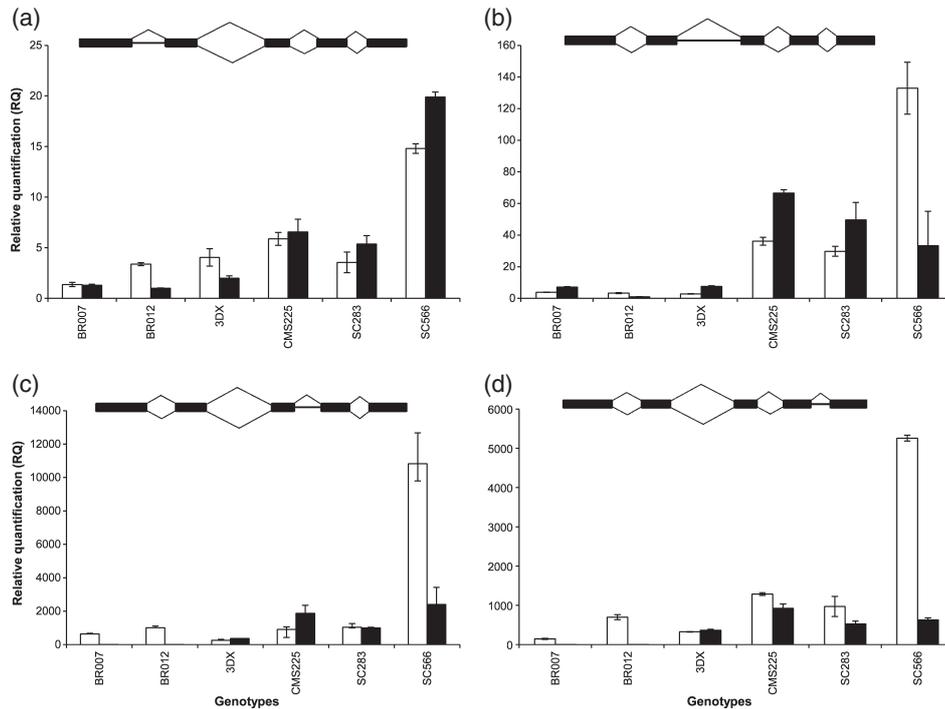
Figure 7. Expression analysis of *SbMATE* alternative transcripts.
Relative quantification of expression of *SbMATE* isoforms was performed in seedlings grown in nutrient solution without (white bars) or with 27 μM Al^{3+} (black bars) (pH 4.0) for 6 days. Intron-specific primers were designed for alternative transcripts (shown schematically at the top of each panel) retaining introns 1 (a), 2 (b), 3 (c) and 4 (d). Expression in the Al-sensitive line, BR012, was used as the reference. Values are means ± SD of three replicates.

such, our data imply the importance of regulatory factors acting *in cis* within the *Alt$_{SB}$* locus, leading to a broad spectrum of Al-tolerance phenotypes. Examples of *cis*-acting regulatory elements influencing flowering time and plant architecture have been reported for the maize (*Zea mays*) loci *Vgt1* (Salvi *et al.*, 2007) and *tb1*, respectively (Clark *et al.*, 2006; Studer *et al.*, 2011). In addition, *cis*-acting elements altering Al-tolerance gene expression have been reported for *TaALMT1* in wheat (Ryan *et al.*, 2010b) and *HvAACT1* in barley (Fujii *et al.*, 2012). For *SbMATE* in sorghum, repeat variations within a *Tourist*-like miniature inverted-repeat transposable element (MITE) inserted in the promoter region correlated with aluminum tolerance in various sorghum lines, suggesting that these repeats harbor *cis* elements that enhance *SbMATE* expression and thus Al tolerance (Magalhaes *et al.*, 2007).

However, the present data also indicate that *SbMATE* expression is regulated at multiple levels, and the relative importance of each component depends on the genetic context, i.e. the findings presented here suggest that *SbMATE* expression depends on the *Alt$_{SB}$* donor allele and also on *trans*-acting factors that are located outside the introgression region in the NILs. The importance of foreign *trans*-acting factors is emphasized by the parallel reduction in both *SbMATE* expression and Al tolerance in NILs in which only the region harboring *Alt$_{SB}$* was introgressed, compared to the respective parents, resulting in introgres-

sion lines that were always less tolerant than the original parents. The increase in the correlation between *SbMATE* expression and Al tolerance from 0.6 in the parents to 0.9 in the NILs suggest that distinctly different Al-tolerant genes to *SbMATE* may also contribute to the Al tolerance displayed by the parents, as previously reported (Caniato *et al.*, 2007). However, the fact that NILs derived from the very Al-tolerant lines SC566 and SC283 were still highly Al-tolerant suggests a minor effect of additional Al-tolerance genes compared to that conferred by *Alt$_{SB}$*, at least in highly Al-tolerant donors.

The model shown in Figure S4 depicts the joint role of *cis* and *trans* effects in controlling *SbMATE* expression in sorghum, emphasizing the dominance of *cis* effects in explaining differential levels of *SbMATE* expression, and the reduction of *SbMATE* expression in NILs due to loss of *trans*-acting factors. Recent published data suggest that changes in both *cis* and *trans* factors are responsible for overall regulation of gene expression (Shi *et al.*, 2012). Consistent with our findings indicating dominance of *cis* effects in explaining the variation in *SbMATE* expression, expression divergence between species, including Arabidopsis, appears to be more influenced by *cis* effects (Kuo *et al.*, 2010). This may result from the high plasticity of *cis*-regulatory regions, while transcription factors, for example, may evolve at a comparatively slower rate (Wray, 2007; Kuo *et al.*, 2010). Our model suggests that there is

compensatory evolution of *cis* factors in highly Al-tolerant lines such as SC566, which conceivably enables maintenance of high *SbMATE* expression despite deleterious allelic variation at *trans*-factor loci. As a precedent, Tsong *et al.*, (2006) reported specific and sequential changes in both *cis*- and *trans*-regulatory elements, resulting in a shift from positive to negative regulation of genes involved with mating type in yeast. In addition, an instance of coordinated evolution between a DNA-binding transcription factor and its *cis*-regulatory site was reported in yeast, leading to a 'regulatory homeostasis' scenario whereby mutations in *cis* and *trans* factors occur in a compensatory fashion to maintain transcriptional regulation (Kuo *et al.*, 2010).

Genetic background effects related to Al tolerance have been reported (reviewed by Magalhaes, 2006). Similar to the case in sorghum, Johnson *et al.*, (1997) observed incomplete transfer of Al tolerance in wheat NILs, which was hypothesized to be the result of the loss of additional genes present in the parent or reduced expression of Al tolerance in the hard red winter genetic background. In Arabidopsis, Hoekenga *et al.*, (2006) also observed genetic background effects related to *AtALMT1*. It is tempting to speculate that the association between Al tolerance and gene expression typically observed for genes belonging to the MATE and ALMT families (reviewed by Delhaize *et al.*, 2012) involves a number of master switches. Mutations at these accessory loci may lead to the reduction or loss of regulatory function in a given genetic context, resulting in frustrated expectations when only the transporter loci are targeted in NIL development. As suggested by Delhaize *et al.*, (2012), the existence of multiple genes acting within common physiological mechanisms may reconcile a possible paradox regarding the apparently large number of genes involved in Al tolerance in rice and Arabidopsis. A possible candidate for a transcription factor affecting *SbMATE* expression is a sorghum homolog of *STOP1*, which, at least in Arabidopsis (Iuchi *et al.*, 2007) and rice (Yamaji *et al.*, 2009), has been shown to influence the expression of Al-tolerance genes. However, we used quantitative RT–PCR to study the expression of the best hit in sorghum (Sb03g041170) for Arabidopsis STOP1 (At1g34370), and did not observe a consistent decrease in expression in the NILs compared to the parents. This suggests that additional, as yet unidentified, regulatory loci are involved in reduced *SbMATE* expression in sorghum.

Sequence alignment for various sorghum genotypes, including highly Al-sensitive and Al-tolerant lines, uncovered the strikingly monomorphic nature of the *SbMATE* coding region in sorghum, with highly Al-sensitive and Al-tolerant lines, such as BR007 and SC283, showing identical *SbMATE* haplotypes. Therefore, as observed for *TaALMT1* in wheat (Sasaki *et al.*, 2006) and *HvAACT1* in barley (Furukawa *et al.*, 2007), SNPs located in the coding region do not appear to explain differences in Al tolerance,

reinforcing the importance of regulatory loci in Al tolerance conferred by *SbMATE*. Nevertheless, the only coding region polymorphisms found were coincidental with the extremely Al-sensitive and Al-tolerant phenotypes in Tx642 and SC566, respectively. A premature stop codon in Tx642 probably leads to complete loss of SbMATE function and extreme Al sensitivity. In SC566, electrophysiological analysis of SbMATE L261H did not support a role for the His residue at position 261 in its high citrate release rate that is not inhibited even at high Al^{3+} activities in nutrient solution. Alternatively, given its peripheral orientation towards the lipid bilayer, this residue may be involved in the transporter's regulation *in planta*, via indirect mechanism(s) involving other interacting proteins that are absent in the heterologous expression system. However, we cannot rule out the possibility that the pattern of citrate release observed in SC566 is solely due to its high *SbMATE* expression level.

This study reports on the occurrence of extensive alternative splicing in *SbMATE* transcripts. In humans, *hMATE2–K* was found to be due to alternative splicing of *hMATE2*, and results in organ-specific expression patterns leading to functional divergence (Masuda *et al.*, 2006). In the current study, intron retention was observed for *SbMATE* alternative transcripts, consistent with the high frequency of this event reported in Arabidopsis (Filichkin *et al.*, 2010). Although the fact that all alternative *SbMATE* transcripts were found to contain premature termination codons raises questions with regards to the functionality of the various isoforms in citrate transport, the observed higher expression of *SbMATE* isoforms in Al-tolerant versus Al-sensitive lines suggests a possible role for alternative splicing in regulating *SbMATE* expression and differential Al tolerance.

Given the position of the premature termination codons in *SbMATE*, all isoforms except the intron 3-retaining isoform may ultimately be degraded via nonsense-mediated RNA decay, which is a quality control-based surveillance mechanism that avoids the production of truncated proteins (Maquat, 2004; Hori and Watanabe, 2005). Coupling of alternative splicing and nonsense-mediated RNA decay is now viewed as a possibly important mechanism that helps regulate gene expression (Hillman *et al.*, 2004; Kalyna *et al.*, 2011). As shown here in Figure 3 and observed in our previous study (Magalhaes *et al.*, 2007), *SbMATE* is also expressed in the absence of Al. In both the presence and absence of Al, *SbMATE* expression in sorghum is localized to the epidermis and outer cortical cells of the root apex. Thus the spatial localization of *SbMATE* expression is unlike that of its homolog in barley, *HvAACT1*. In barley, *HvAACT1* encodes the root Al-activated citrate efflux transporter in Al-tolerant barley lines (Fujii *et al.*, 2012). However, unlike SbMATE, HvAACT1 functions primarily as a transporter localized to root pericycle cells,

where it releases citrate to the xylem for the transport of iron to the shoot. Fujii *et al.*, (2012) found that, in Al-tolerant barley lines, there is a 1 kb insertion upstream of the *HvAACT1* coding region that changes the location of *HvAACT* expression from the root stele to the epidermis and outer cortex of root tips, where it can also transport citrate into the rhizosphere for Al tolerance. The moderately high level of *SbMATE* transcripts in sorghum roots in the absence of Al may not be translated into functional protein, as it is possible that SbMATE translation under these conditions may impose an undesirable energy cost and be detrimental to Al-tolerant lines when cultivated in soils without Al toxicity.

Interestingly, a link between stress factors and alternative splicing has been reported (Iida *et al.*, 2004; Ner-Gaon *et al.*, 2004; Nakaminami *et al.*, 2011). Therefore, it is possible that, in avoiding the production of truncated proteins with possibly no functional role in Al-induced citrate release, nonsense-mediated RNA decay may contribute to a more efficient use of energy under Al stress, without reduced fitness in non-stress environments. In fact, nonsense-mediated RNA decay has been hypothesized to be a means to rapidly switch off gene expression (Neu-Yilik *et al.*, 2004). At this time, this possibility is highly speculative, and further investigations are needed to clarify the possible role of alternative splicing and nonsense-mediated RNA decay in differential Al tolerance.

This study indicates that reduced *SbMATE* expression gives rise to potentially strong genetic background effects that may reduce the efficiency of molecular breeding approaches aimed at enhancing sorghum Al tolerance based on the Alt_{SB} locus. Possibly due to the nature of the *cis*-acting sequences, the Alt_{SB} locus from certain highly Al-tolerant sources, namely SC283 and SC566, control a significant proportion of the Al-tolerance phenotype. Therefore, choice of donor lines in molecular breeding programs should be based not only on the Al-tolerance phenotype but also on sustained *SbMATE* expression in various genetic backgrounds. While the existence of *trans*-acting factors creates difficulties for allele mining approaches aimed at isolating highly Al-tolerant lines based solely on *SbMATE* haplotype information, they offer the potential to explore transgressive segregation for Al tolerance in sorghum. This justifies our current efforts to isolate the genetic factors affecting *SbMATE* expression, enabling their exploitation in molecular breeding approaches aimed at improved yield performance for sorghum cultivated on acid, Al-toxic soils.

EXPERIMENTAL PROCEDURES

Plant materials

Near-isogenic lines were developed by marker-assisted backcrossing to introgress the Alt_{SB} locus from the various parents using the Al-sensitive line BR012 as common recurrent parent.

BC$_3$(F$_{3-8}$) NILs fixed for the Alt_{SB} donor alleles were generated using foreground selection for markers S17, S73, CTG29 and M181 previously described by Caniato *et al.*, (2007, 2011). Three additional backcross generations were used for the CMS225 NIL. As these flanking markers show extremely tight genetic and physical linkage to Alt_{SB} (Caniato *et al.*, 2007, 2011), recombination events are not expected given the population sizes used here. In fact, we sequenced amplicons spanning polymorphic regions between each parent to confirm fixation of the donor alleles in the NILs.

Determination of root citrate exudation in sorghum lines

Seed surface sterilization, germination and seedling growth conditions were as described below for hydroponic analysis of Al tolerance. For citrate exudation experiments, after 24 h of stabilization in nutrient solution without Al, the solution was changed to either control ($-$Al) nutrient solution or nutrient solution containing 11, 20, 27 or 39 μM Al^{3+} (values indicate Al^{3+} activity estimated using the speciation software GEOCHEM–PC, Parker *et al.*, 1995). Each experimental unit consisted of six seedlings, and five replications were performed. After 5 days, root exudate collection began by transferring six seedlings per genotype to 50 ml plastic centrifuge tubes containing 4.3 mM CaCl$_2$·6 H$_2$O, without or with Al added as AlCl$_3$·6 H$_2$O at pH 4.5. The same free Al^{3+} activities as used when seedlings were grown in the complete nutrient solution were used for collection of root exudates. Root exudates were collected for 6 h, and the resultant exudation solution was passed through an OnGuard$^{®}$ II Ag anionic silver chromatograph column (Dionex, http://www.dionex.com), and then treated with Dowex$^{®}$ 50WX8 cationic resin (Sigma Aldrich, http://www.sigmaaldrich.com). Subsequently, 1 ml sub-samples were lyophilized and resuspended in 0.1 ml ultrapure water. Organic acid analysis was performed using a capillary electrophoresis system as described by Piñeros *et al.*, (2002).

Hydroponic analysis of aluminum tolerance

Phenotypic analysis of Al tolerance was performed in nutrient solution containing either 0 or 27 μM Al^{3+}, as described by Caniato *et al.*, (2007, 2011). The experiment consisted of a completely randomized design with three replications and seven plants per replication. Briefly, seeds were sterilized with 0.525% NaOCl and rinsed with de-ionized water. After 3 days of germination, seedlings were transferred to polyethylene cups placed into containers filled with 8 L of nutrient solution lacking Al at pH 4.0, under aeration, and placed in a growth chamber with 27°C day and 20°C night temperatures, a light intensity of 330 μmol photons m^{-2} sec^{-1} and a 12 h photoperiod. After 24 h of acclimation, the initial length of each seedling's root growing in control solution (IL$_c$) was measured. The solution was then replaced by nutrient solution of identical composition but containing either no Al or 27 μM Al^{3+} supplied as AlK(SO$_4$)$_2$·12 H$_2$O. Final root lengths under Al treatment (FL$_{Al}$) or control solution (FL$_c$) were obtained after 5 days of exposure to Al. For each inbred line, mean values for relative percentage net root growth (RNRG) at 27 μM Al^{3+}, were estimated by dividing the net root growth under Al treatment (FL$_{Al}$ $-$ IL$_c$) by the net root growth without Al (FL$_c$ $-$ IL$_c$).

Analysis of *SbMATE* expression in sorghum lines and NILs

Sorghum seedlings were grown using the same methods used for assessment of Al tolerance in nutrient solution. Each experimental unit consisted of the first centimeter of root apices collected from 28 intact plants after 5 days of Al treatment. The tissue was col-

lected and immediately frozen in liquid N_2. Total RNA was extracted using an RNeasy plant mini kit (Qiagen, http://www.qiagen.com), and 10 units of RNase-free DNase I (Qiagen) were added to each sample after incubation at room temperature for 15 min. First-strand cDNA was synthesized using 2 μg total RNA with a high-capacity cDNA reverse transcription kit (Applied Biosystems, http://www.appliedbiosystems.com).

SbMATE transcripts were quantified using a TaqMan gene expression kit on an ABI Prism 7500 real-time PCR system (Applied Biosystems). A series of cDNA dilutions were used to create standard curves for both *SbMATE* transcripts and 18S rRNA, which was used as the endogenous control. Then, the selected dilutions for specific cDNA samples (10 ng for *SbMATE* transcripts and 0.01 ng for 18S rRNA) were used as real-time PCR templates to quantify relative transcript levels according to the manufacturer's instructions. The forward and reverse primers are 5′-CAGCCATTGCCCATGTTCTTT-3′ and 5′-ACCAGCTTGCTCAGCATTATCA-3′, respectively, and the probe sequence is 6FAM CCCAGTACCTGATAACGC TAMRA. Levels of expression for endogenous 18S rRNA were determined using TaqMan ribosomal RNA control reagents (Applied Biosystems). Reactions with distilled water were used as negative controls. Relative quantification was calculated using $\Delta\Delta C_T$ method with the Al-sensitive accession BR012 as calibrator (Schmittgen and Livak, 2008), and three technical replicates were performed.

Analysis of the genomic structure of *SbMATE*

Genomic DNA was isolated from leaf tissue as described by Saghai-Maroof *et al.*, (1984). Complete sequencing of *SbMATE* was performed using the following primer pairs: (i) 5′-CACGTGAGCCTGCATCTTTA-3′ (annealing to the 5′ region) and 5′-GAAGCCGCAGTACCATTCTC-3′ (annealing to exon 1), (ii) 5′-AACAAGTGGCCAAGTGGGTGATCA-3′ (annealing to the 5′ region) and 5′-GGCACGCACAGGCACAGTAACTTA-3′ (annealing to intron 1), (iii) 5′-GGGAACAGGAGGTTCGTGCCGTCC-3′ (annealing to exon 1) and 5′-CCTACTGATCGACTACTGACCGCA-3′ (annealing to the exon 4/intron 4 junction), (iv) 5′-GCCCGCGCTGCGCTACCTGA-3′ (annealing to exon 2) and 5′-CCTACTGATCGACTACTGACCGCA-3′ (annealing to the exon 4/intron 4 junction), (v) 5′-ACGCTGATAATGCTGAGCAAGCTG-3′ (annealing to exon 4) and 5′-ACGTACTAGGGTCGTTTGGGTTGT-3′ (annealing to the 3′ region).

PCR fragments were resolved in 1% agarose gels and purified using a QIAquick gel extraction kit (Qiagen). Sequencing reactions were performed using a Big Dye version 3.1 kit (Applied Biosystems) in an ABI PRISM 3100 genetic analyzer (Applied Biosystems) according to the manufacturer's instructions. Sequences were aligned using CLUSTAL W (Thompson *et al.*, 1994).

Functional characterization of SbMATE and SbMATE L261H in *Xenopus* oocytes

cRNAs were prepared using an Ambion® mMessage mMachine® T7 *in vitro* transcription kit (Invitrogen, www.invitrogen.com) from 1 μg of *Sca*I-linearized T7TS plasmid template containing the SbMATE or SbMATE L261H coding region, flanked by the 3′- and 5′-untranslated regions of a *Xenopus* β–globin gene. Harvesting of *Xenopus laevis* oocytes, micro-injection and whole-cell recordings under two-electrode voltage clamp were performed as described previously (Piñeros *et al.*, 2008). Briefly, stage V–VI oocytes were injected with 48 nl water containing 20 ng of cRNA encoding SbMATE or SbMATE L261H. Whole-cell currents were recorded for 2–3 days after the micro-injections using an Axoclamp 900A amplifier/PClamp 10 data acquisition system (Molecular Devices http://moleculardevices.com). Recordings were performed under voltage clamp in a solution consisting of 48 mM NaCl, 1 mM KCl and 0.8 mM $CaCl_2$, adjusted to 195 mOsmol using sorbitol. The pH of the solution was adjusted to pH 7.5 or 4.5 as indicated in the figure legends. The holding potential was set to 0 mV, and voltage test pulses (2.5 sec duration) were step-increased from +40 mV to −140 mV (in 20 mV increments), with a 7.5 sec resting phase at 0 mV between each voltage pulse. The current/voltage (I/V) relationships were determined by measuring the current amplitude at the end of the test pulses. Recordings were performed using two biological replicates (i.e. two frog donors).

Alternative splicing of *SbMATE*

Genomic DNA and cDNA from each sorghum line were used as templates with primers EXON-1R 5′- CAGGTCATGAAGGTGTGCAT-3′ and EXON-2F 5′-CTTGCATGGCGAGAGACAG-3′ or EXON-5F 5′-GAACTGCAGCCCGAGTCC-3′. Amplifications were performed in a 20 μl reaction that contained 30 ng genomic DNA or 3 μl cDNA, 10 × Taq reaction buffer, 0.5 mM dNTP, 2 mM $MgCl_2$, 10 pmol of each primer, 5% dimethyl sulfoxide and 0.5 units of Taq DNA polymerase (Invitrogen). Amplification proceeded with an initial denaturation step of 95°C for 2 min, followed by 40 cycles at 94°C for 30 sec, 57°C for 30 sec and 72°C for 2 min and 30 sec, with a final extension step at 72°C for 5 min. PCR products were resolved in a 1.5% agarose gel, and extracted from the gel using a QIAquick gel extraction kit (Qiagen) according to the manufacturer's instructions. PCR fragments were subsequently cloned into the pGEM®–T Easy vector (Promega, http://www.promega.com) and sequenced using M13 primers as described for *SbMATE* sequencing above.

In order to analyze expression of the various splice variants of *SbMATE*, seedlings were grown in nutrient solution at pH 4.0 with or without 27 μM Al^{3+}. The first centimeter of 14 root tips per genotype was collected after 1, 3 and 6 days of Al exposure. Total RNA was isolated using an RNeasy plant mini kit (Qiagen), and cDNA was obtained using a high-capacity cDNA reverse transcription kit (Applied Biosystems). The following primers that anneal to each of the *SbMATE* introns were used: INTRON–1F, 5′-TGCACCGACGAATCTAGTTCAC-3′ and INTRON–1R, 5′-GCGTCAAGCCGGTAAGTTACTG-3′; INTRON–2F, 5′-GACATGTGTCCTTACTCTCTCATCCA-3′ and INTRON–2R, 5′-CGCTTTGAGATGTGTGTTTGC-3′; INTRON–3F, 5′-CATGACCACCGCATCTCCTT-3′ and INTRON–3R, 5′-GTCAGTTGTTGCGGCCAAT-3′; INTRON–4F, 5′-TCCATTAACAAGACGAGATGATGAC-3′ and INTRON–4R, 5′-TGCCAGCAGAAGGAATCCTATAC-3′. Quantitative real-time PCR was performed using an ABI Prism 7500 real-time PCR system (Applied Biosystems) as follows: each PCR reaction contained the selected dilution for specific cDNA samples (5 ng for *SbMATE* transcripts and 0.005 ng for 18S rRNA), 0.25 μM of each primer and 5 μl Fast SYBR Green Master Mix (Applied Biosystems) in a final volume of 10 μl. 18S rRNA was used as an endogenous control using the primers 5′-AATCCCTTAACGAGGATCCATTG-3′ and 5′-CGCTATTGGAGCTGGAATTACC-3′. Dissociation curves were generated to ensure amplification of a single target, and relative quantification was calculated using $\Delta\Delta C_T$ method (Schmittgen and Livak, 2008).

Alternative transcripts were confirmed by high-throughput RNA sequencing using the Illumina platform (Illumina, http://www.illumina.com). RNA extraction and strand-specific RNA-seq library preparations were performed as described previously (Zhong *et al.*, 2011). The resulting sequences were aligned to the sorghum genome sequence using Tophat (Trapnell *et al.*, 2009), and visualized using Integrative Genomics Viewer software (Robinson *et al.*, 2011).

ACKNOWLEDGEMENTS

SUPPORTING INFORMATION

Additional Supporting Information may be found in the online version of this article.

Figure S1. Alternative splicing events for *SbMATE* as determined by RNA-seq.

Figure S2. Expression analysis for alternative transcripts for *SbMATE* that retain intron 1.

Figure S3. Expression analysis for alternative transcripts for *SbMATE* that retain intron 1 in parents and NILs.

Figure S4. Bi-factorial model showing the roles of and interaction between *cis* and *trans* effects in regulation of *SbMATE* expression.

REFERENCES

Caniato, F.F., Guimarães, C.T., Schaffert, R.E., Alves, V.M.C., Kochian, L.V., Borém, A., Klein, P.E. and Magalhaes, J.V. (2007) Genetic diversity for aluminum tolerance in sorghum. *Theor. Appl. Genet.* **114**, 863–876.

Caniato, F.F., Guimarães, C.T., Hamblin, M. *et al.* (2011) The relationship between population structure and aluminum tolerance in cultivated sorghum. *PLoS ONE*, **6**, 1–14.

Clark, R.M., Wagler, T.N., Quijada, P. and Doebley, J. (2006) A distant upstream enhancer at the maize domestication gene *tb1* has pleiotropic effects on plant and inflorescent architecture. *Nat. Genet.* **38**, 594–597.

Delhaize, E., Gruber, B.D. and Ryan, P.R. (2007) The roles of organic anion permeases in aluminium resistance and mineral nutrition. *FEBS Lett.* **581**, 2255–2262.

Delhaize, E., Ma, J.F. and Ryan, P.R. (2012) Transcriptional regulation of aluminium tolerance genes. *Trends Plant Sci.* **17**, 341–348.

Filichkin, S.A., Priest, H.D., Givan, S.A., Shen, R., Bryant, D.W., Fox, S.E., Wong, W.-K. and Mockler, T.C. (2010) Genome-wide mapping of alternative splicing in *Arabidopsis thaliana*. *Genome Res.* **20**, 45–58.

Fujii, M., Yokosho, K., Yamaji, N., Saisho, D., Yamane, M., Takahashi, H., Sato, K., Nakazono, M. and Ma, J.F. (2012) Acquisition of aluminium tolerance by modification of a single gene in barley. *Nat. Commun.* **3**, 713.

Furukawa, J., Yamaji, N., Wang, H., Mitani, N., Murata, Y., Sato, K., Katsuhara, M., Takeda, K. and Ma, J.F. (2007) An aluminum-activated citrate transporter in barley. *Plant Cell Physiol.* **48**, 1081–1091.

He, X., Szewczyk, P., Karyakin, A., Evin, M., Hong, W.-X., Zhang, Q. and Chang, G. (2010) Structure of a cation-bound multidrug and toxic compound extrusion transporter. *Nature*, **467**, 991–994.

Hillman, R.T., Green, R.E. and Brenner, S.E. (2004) An unappreciated role for RNA surveillance. *Genome Biol.* **5**, R8.

Hoekenga, O.A., Maron, L.G., Piñeros, M.A. *et al.* (2006) *AtALMT1*, which encodes a malate transporter, is identified as one of several genes critical for aluminum tolerance in Arabidopsis. *Proc. Natl Acad. Sci. USA*, **103**, 9738–9743.

Hori, K. and Watanabe, Y. (2005) UPF3 suppresses aberrant spliced mRNA in Arabidopsis. *Plant J.* **43**, 530–540.

Horst, W.J., Wang, Y. and Eticha, D. (2010) The role of the root apoplast in aluminium-induced inhibition of root elongation and in aluminium resistance of plants: a review. *Ann. Bot.* **106**, 185–197.

Huang, C.F., Yamaji, N., Chen, Z. and Ma, J.F. (2012) A tonoplast-localized half-size ABC transporter is required for internal detoxification of aluminum in rice. *Plant J.* **69**, 857–867.

Iida, K., Seki, M., Sakurai, T., Satou, M., Akiyama, K., Toyoda, T., Konagaya, A. and Shinozaki, K. (2004) Genome-wide analysis of alternative premRNA splicing in *Arabidopsis thaliana* based on full-length cDNA sequences. *Nucleic Acids Res.* **32**, 5096–5103.

Iuchi, S., Koyama, H., Iuchi, A., Kobayashi, Y., Kitabayashi, S., Kobayashi, Y., Ikka, T., Hirayama, T., Shinozaki, K. and Kobayashi, M. (2007) Zinc finger protein STOP1 is critical for proton tolerance in Arabidopsis and coregulates a key gene in aluminum tolerance. *Proc. Natl Acad. Sci. USA*, **104**, 9900–9905.

Johnson, J.P., Carver, B.F. and Baligar, V.C. (1997) Expression of aluminum tolerance transferred from Atlas 66 to Hard winter wheat. *Crop Sci.* **37**, 103–108.

Jones, D.L. and Kochian, L.V. (1995) Aluminum inhibition of the inositol 1,4,5–trisphosphate signal transduction pathway in wheat roots: a role in aluminum toxicity? *Plant Cell*, **7**, 1913–1922.

Kalyna, M., Simpson, C.G., Syed, N.H. *et al.* (2011) Alternative splicing and nonsense-mediated decay modulate expression of important regulatory genes in Arabidopsis. *Nucleic Acids Res.* **40**, 1–16.

Kelley, L. and Sternberg, M.J.E. (2009) Protein structure prediction on the web: a case study using the Phyre server. *Nat. Protoc.* **4**, 363–371.

Kinraide, T.B., Parker, D.R. and Zobel, R.W. (2005) Organic acid secretion as a mechanism of aluminium resistance: a model incorporating the root cortex, epidermis, and the external unstirred layer. *J. Exp. Bot.* **56**, 1853–1865.

Kochian, L.V., Hoekenga, O.A. and Pineros, M.A. (2004) How do crop plants tolerate acid soils? Mechanisms of aluminum tolerance and phosphorus efficiency. *Annu. Rev. Plant Biol.* **55**, 459–493.

Kochian, L.V., Piñeros, M.A. and Hoekenga, O.A. (2005) The physiology, genetics and molecular biology of plant aluminum resistance and toxicity. *Plant Soil*, **274**, 175–195.

Kuo, D., Licon, K., Bandyopadhyay, S., Chuang, R., Luo, C., Catalana, J., Ravasi, T., Tan, K. and Ideker, T. (2010) Coevolution within a transcriptional network by compensatory *trans* and *cis* mutations. *Genome Res.* **20**, 1672–1678.

Liu, J., Magalhaes, J.V., Shaff, J. and Kochian, L.V. (2009) Aluminum-activated citrate and malate transporters from the MATE and ALMT families function independently to confer Arabidopsis aluminum tolerance. *Plant J.* **57**, 389–399.

Ma, J.F., Ryan, P.R. and Delhaize, E. (2001) Aluminium tolerance in plants and the complexing role of organic acids. *Trends Plant Sci.* **6**, 273–278.

Magalhaes, J.V. (2006) Aluminum tolerance genes are conserved between monocots and dicots. *Proc. Natl Acad. Sci. USA*, **103**, 9749–9750.

Magalhaes, J.V., Garvin, D.F., Wang, Y., Sorrells, M.E., Klein, P.E., Schaffert, R.E. and Kochian, L.V. (2004) Comparative mapping of a major aluminum tolerance gene in sorghum and other species in the Poaceae. *Genetics*, **167**, 1905–1914.

Magalhaes, J.V., Liu, J., Guimarães, C.T. *et al.* (2007) A gene in the multidrug and toxic compound extrusion (MATE) family confers aluminum tolerance in sorghum. *Nat. Genet.* **39**, 1156–1161.

Maquat, L.E. (2004) Nonsense-mediated mRNA decay: splicing, translation and mRNP dynamics. *Nat. Rev. Mol. Cell Biol.* **5**, 89–99.

Masuda, S., Terada, T., Yonezawa, A., Tanihara, Y., Kishimoto, K., Katsura, T., Ogawa, O. and Inui, K. (2006) Identification and functional characterization of a new human kidney-specific H⁺/organic cation antiporter, kidney-specific multidrug and toxin extrusion 2. *J. Am. Soc. Nephrol.* **17**, 2127–2135.

Nakaminami, K., Matsui, A., Shinozaki, K. and Seki, M. (2011) RNA regulation in plant abiotic stress responses. *Biochim. Biophys. Acta*, **1819**, 149–153.

Ner-Gaon, H., Halachmi, R., Savaldi-Goldstein, S., Rubin, E., Ophir, R. and Fluhr, R. (2004) Intron retention is a major phenomenon in alternative splicing in Arabidopsis. *Plant J.* **39**, 877–885.

Neu-Yilik, G., Gehring, N.H., Hentze, M.W. and Kulozik, A.E. (2004) Nonsense-mediated mRNA decay: from vacuum cleaner to Swiss army knife. *Genome Biol.* **5**, 218.

Parker, D.R., Norvell, W.A. and Chaney, R.L. (1995) GEOCHEM-PC: a chemical speciation program for IBM and compatible computers. In *Chemical Equilibrium and Reaction Models* (Leoppert, R., Schwab, A. and Goldberg, S., eds). Madison, WI: Soil Science Society of America, pp. 253–269.

Piñeros, M.A., Magalhaes, J.V., Carvalho Alves, V.M. and Kochian, L.V. (2002) The physiology and biophysics of an aluminum tolerance mechanism based on root citrate exudation in maize. *Plant Physiol.* **129**, 1194–1206.

Piñeros, M.A., Cancado, G.M.A. and Kochian, L.V. (2008) Novel properties of the wheat aluminum tolerance organic acid transporter (TaALMT1) revealed by electrophysiological characterization in *Xenopus oocytes*: functional and structural implications. *Plant Physiol.* **147**, 2131–2146.

Robinson, J.T., Thorvaldsdóttir, H., Winckler, W., Guttman, M., Lander, E.S., Getz, G. and Mesirov, J.P. (2011) Integrative genomics viewer. *Nat. Biotechnol.* **29**, 24–26.

Ryan, P.R., Tyerman, S.D., Sasaki, T., Furuichi, T., Yamamoto, Y., Zhang, W.H. and Delhaize, E. (2010a) The identification of aluminium-resistance genes provides opportunities for enhancing crop production on acid soils. *J. Exp. Bot.* **62**, 9–20.

Ryan, P.R., Raman, H., Gupta, S., Sasaki, T., Yamamoto, Y. and Delhaize, E. (2010b) The multiple origins of aluminium resistance in hexaploid wheat include *Aegilops tauschii* and more recent *cis* mutations to *TaALMT1*. *Plant J.* **64**, 446–455.

Saghai-Maroof, M.A., Soliman, K.A., Jorgensen, R.A. and Allard, R.W. (1984) Ribossomal DNA spacer lenght polymorphism in barley: mendelian inheritance, chromosomal location and populations dynamics. *Proc. Natl. Acad. Sci. USA*, **81**, 8014–8018.

Salvi, S., Sponza, G., Morgante, M. *et al.* (2007) Conserved noncoding genomic sequences associated with a flowering-time quantitative trait locus in maize. *Proc. Natl Acad. Sci. USA*, **104**, 11376–11381.

Sasaki, T., Yamamoto, Y., Ezaki, B., Katsuhara, M., Ahn, S.J., Ryan, P.R., Delhaize, E. and Matsumoto, H. (2004) A wheat gene encoding an aluminum-activated malate transporter. *Plant J.* **37**, 645–653.

Sasaki, T., Ryan, P.R., Delhaize, E., Hebb, D.M., Ogihara, Y., Kawaura, K., Noda, K., Kojima, T., Toyoda, A., Matsumoto, H. and Yamamoto, Y. (2006) Sequence upstream of the wheat (*Triticum aestivum* L.) *ALMT1* gene and its relationship to aluminum resistance. *Plant Cell Physiol.* **47**, 1343–1354.

Schmittgen, T.D. and Livak, K.J. (2008) Analyzing real-time PCR data by the comparative C_T method. *Nat. Protoc.* **3**, 1101–1108.

Shi, X., Ng, D.W.-K., Zhang, C., Comai, L., Ye, W. and Chen, J.Z. (2012) *Cis*- and *trans*-regulatory divergence between progenitor species determines gene-expression novelty in *Arabidopsis* allopolyploids. *Nat. Commun.* **3**, 950.

Studer, A., Zhao, Q., Ross-Ibarra, J. and Doebley, J. (2011) Identification of a functional transposon insertion in the maize domestication gene *tb1*. *Nat. Genet.* **43**, 1160–1163.

Thompson, J.D., Higgins, D.G. and Gibson, T.J. (1994) CLUSTAL W: improving the sensitivity of progressive multiple sequence alignment through sequence weighting, position-specific gap penalties and weight matrix choice. *Nucleic Acids Res.* **22**, 4673–4680.

Trapnell, C., Pachter, L. and Salzberg, S.L. (2009) TopHat: discovering splice junctions with RNASeq. *Bioinformatics*, **25**, 1105–1111.

Tsong, A.E., Tuch, B.B., Li, H. and Johnson, A.D. (2006) Evolution of alternative transcriptional circuits with identical logic. *Nature*, **443**, 415–420.

von Uexküll, H.R. and Mutert, E. (1995) Global extent, development and economic impact of acid soils. *Plant Soil*, **171**, 1–15.

Wray, G.A. (2007) The evolutionary significance of *cis*-regulatory mutations. *Nat. Rev. Genet.* **8**, 206–216.

Xia, J., Yamaji, N., Kasai, T. and Ma, J.F. (2010) Plasma membrane-localized transporter for aluminum in rice. *Proc. Natl Acad. Sci. USA*, **107**, 18381–18385.

Yamaji, N., Huang, C.F., Nagao, S., Yano, M., Sato, Y., Nagamura, Y. and Ma, J.F. (2009) A zinc finger transcription factor ART1 regulates multiple genes implicated in aluminum tolerance in rice. *Plant Cell*, **21**, 3339–3349.

Yokosho, K., Yamaji, N. and Ma, J.F. (2011) An Al-inducible MATE gene is involved in external detoxification of Al in rice. *Plant J.* **68**, 1061–1069.

Zhong, S., Joung, J.G., Zheng, Y., Chen, Y.R., Liu, B., Shao, Y., Xiang, J.Z., Fei, Z. and Giovannoni, J.J. (2011) High-throughput Illumina strand-specific RNA sequencing library preparation. *Cold Spring Harb. Protoc.* **2011**, 940–949.